Pinpointing land and surface air temperature variability across topographies in Washington via spatial joining of spaceborne and terrestrial data

Submitted as partial fulfilment of a Master's of Science in Geospatial Technologies

Eric M. Anderson[1]

[1]University of Washington at Tacoma, 1900 Commerce St, Tacoma, WA 98402
Email: ermian98@uw.edu

Abstract

Digital weather apps that provide near-real time temperature data often receive data from a few regional weather stations. On cloudless days, temperature varies greatly between topographies, rendering these apps inaccurate depending on the geographical coordinates queried. This research project partially corrects this by measuring the degree to which four predictor variables (season, land cover type, shadow, sun altitude) displace land surface temperature (LST) from surface air temperature (SAT) on cloudless days. To determine this correction, terrestrial weather data from 4,767 Weather Underground (WU) personal weather stations (PWS) in Washington State between June 2020 and 2021 were joined with remotely sensed LST data from the ECOsystem Spaceborne Thermal Radiometer Experiment on Space Station (ECOSTRESS) sensor at a 70-meter spatial resolution. These joined data produced temperature "penalties" (LST minus SAT) for all 1,218 predictor variable permutations, which were validated via bagging ("bootstrap aggregating") and applied to the 70-meter LST grid. After penalty correction, the absolute difference between LST and SAT shrunk by 35.7%, with 69.8% of observations reporting a more accurate SAT than before correction. These corrections were stronger during summer, under a high-altitude sun, and on developed land, supporting related research of the urban heat island (UHI) effect. Knowledge of these corrections may enable future researchers to model surface or air temperature when localized data are unavailable (e.g., no satellite or terrestrial data measurements at that particular space/time). These corrections may also help scientists identify causes of unusually hot or cold areas that may have been overlooked in broader climate studies.

Keywords

- Land Surface Temperature (LST)
- Surface Air Temperature (SAT)
- Land Use Land Cover (LULC)
- Spatio-Temporality
- Remote Sensing
- ECOsystem Spaceborne Thermal Radiometer Experiment on Space Station (ECOSTRESS)

1. Introduction

This project utilizes many applications of remote sensing, the acquisition of electromagnetic radiation from distant sensors such as those mounted on Earth observing satellites. A commonly observed band of the electromagnetic spectrum is the thermal infrared (TIR) band. This band is useful for its ability to measure an object's reflected and/or emitted energy on the Earth's surface that is otherwise undetectable by visual light optics like the human retina. Deriving atmospherically corrected land surface temperature (LST) from solar radiant emittance is one application of TIR-band data acquisition, and is necessary for this project.

Some remote sensing endeavors require simultaneous collection of ground-truth data, or "on-the-ground" measurements, to ensure proper instrument calibration and robustness of data analysis for policymaking (Eliezer *et al.* 2019). For this project, the inclusion of terrestrial weather station data at 5-minute intervals from Weather Underground is essential for modelling surface air temperature (SAT) from the ECOSTRESS land surface temperature. Since ground-truth data is collected at discrete coordinate points, unlike continuous remotely sensed data, ground data points are distributed as evenly as possible across diverse land cover types, to capture maximum variation in the data. Crowdsourced data not only accomplish this the best by accounting for human activity across all terrains, but also by confirming the legitimacy of official meteorological reporting stations, such as those at airports (Vetner *et al.* 2020).

Weather satellites equipped with microwave spectrometers have consistently measured and calculated Earth sea surface temperatures since 1969. Within a decade, land surface temperature measurement became routine as well, though more difficult because land emits noisier radiation than water (Yates 1970). Within another decade, atmospheric temperature measurement became commonplace. Today, a great deal of Earth surface temperature measurements are global in scale, contrasting this project's use of high spatial resolution data. Even the more well-known granular temperature sensors, such as the Visible Infrared Imaging Radiometer Suite (VIIRS) and the Moderate Resolution Imaging Spectroradiometer (MODIS), at best produce a grid as sharp as 250x250 meters. Micro-scale surface temperature research primarily concentrates on annual heat patterns in well-populated industrialized areas and seasonal heat patterns across disturbed and undisturbed ecosystems.

The predictor variables of surface air temperature chosen for this project are inspired by a 2008 study that appointed geographical variables (altitude, continentality, etc.) and remote sensing variables (albedo, LST, etc.) to ground-based meteorological stations. The study concluded that both in tandem could significantly predict air temperature 87% of the time, with LST being the most important variable (Cristóbal, Ninyerola, & Pons 2008). More advanced spatial data have become available since this study was published, which is why this project adds land cover and hillshade as geographic variables, retains LST as the remote sensing variable, and summarizes by season. Nonetheless, the methods of interpolating temperature in the 2008 study were followed closely to account for the 36-hour gap between ECOSTRESS flyovers, when remotely sensed data are inaccessible.

Where this project deviates from more conventional surface temperature research is that it analyzes unusually high spatial resolution data across all known temperature zones in Washington, instead of restricting itself to one zone, such as an urban center. The idea is to compare these known temperature zones with the variations between the zones, in pursuit of unearthing tiny, yet ubiquitous regions that exhibit surprising thermal characteristics. This project aims to find the most skewed surface air temperatures from those reported by nearby

weather stations (dubbed "hot" and "cold" spots), and the spatial-temporal correlations for their skew. Finally, this project aims to synthesize these findings to assess the impacts on regional climate change and public well-being. Recognizing such spatio-temporalities will provide climate researchers with another angle to assess and predict local temperature patterns.

2. Methods

To accomplish the aforementioned goals, this project relied profusely on the use of task automation in the Python and R programming languages. Python was selected for its close relationship with the ArcGIS platform (which is also used) and its relatively simple and versatile implementation of geoprocessing tools via the *arcpy* library, native to ArcGIS. Likewise, R was selected for its simplicity to code complex mathematical computations. Before writing such code, careful consideration of the differences between spaceborne and terrestrial data was made. A balance of strong spatial resolution, temporal resolution, and radiometric resolution must be established to regulate the runtime of the computer programs.

2.1 Web Harvesting in R and Preliminary Data Processing

To identify topography on the finest scale, the remotely sensed land surface temperatures were obtained from the ECOsystem Spaceborne Thermal Radiometer Experiment on Space Station (ECOSTRESS) sensor, which provides 70-meter spatial resolution over Washington roughly every 36 hours (derived from Cawse-Nicholson & Anderson 2018). The ECOSTRESS mission began in 2018 and will continue through 2021, covering this project's one-year study period from June 2020 to June 2021. The necessary data were filtered out and batch downloaded from the NASA Earthdata LPDAAC website under the product designations ECO2LSTE, ECO2CLD, and ECO1BGEO. Each were packaged as Hierarchical Data Format (HDF5) files, with the first containing land surface temperature fields (in Kelvin), the second containing probable cloud mask, and the latter containing solar azimuth, zenith, latitude, and longitude fields. A publicly available Python script[4] was run to georeference ECO2LSTE and ECO2CLD using ECO1BGEO. This converted them into the Tagged Image File Format (.tiff), with 32-bit and 6-bit pixels denoting land surface temperature and cloud mask, respectively.

After acquiring the download links for the spaceborne data, the terrestrial data points were collected by programmatically iterating through all Weather Underground (WU) personal weather stations in Washington. This iteration was accomplished via a custom web harvesting script in R, utilizing the *RSelenium* package. Latitude and longitude (to the thousands place) and station ID for all licensed stations during the study period were pulled from the WU website[5] and compiled into a comma-separated values (.csv) file. Stations deemed offline at the beginning, middle, and end of the study period were discarded. Stations deemed online (of which there were 5,323) were spatially joined with each .tiff file in the section 2.2. Those within the extent of a .tiff file had their historical air temperature data at the time of ECOSTRESS flyover harvested from the WU website via the R script.

Additional data for this project included: a 2016 Washington State land cover raster from the National Land Cover Database; a 2013 one arc-second digital elevation model (DEM) from

the Terra ASTER satellite; and Washington municipal and state boundary shapefiles from the WA Department of Transportation website.

2.2 Automated Geospatial Analysis in Python

This next phase in the automation was controlled by Python and was by far the lengthiest, as it was constantly downloading data in excess of 2GB, deleting it, and shuffling it around in RAM as it performed the desired geoprocesses. For each ECOSTRESS flyby reported in Washington during the study period (approximately 1,200), the following analysis was repeated.

The probable cloud mask data from ECO2CLD underwent pixel reclassification to nullify the ECO2LSTE pixels with high cloud probability. Although this often removed a sizeable chunk of the flyby data, this was a crucial step. Clouds scatter the rays absorbed by the ECOSTRESS sensor, meaning that the radiation returned to the sensor would be more indicative of the cloud than of the surface. This reformatted file had its units converted from Kelvin to Fahrenheit, its null values omitted, and its boundary clipped to Washington state to create a compact raster layer, and was saved in a file geodatabase. Meanwhile, a hillshade model for the flyby was approximated using the solar azimuth and zenith angles corresponding to the centroid of the ECO1BGEO file, in order to apply a shadow = yes or no field to each pixel.

Next, the online terrestrial weather stations that overlapped a pixel from the modified ECO2LSTE file were spatially joined to that file and isolated in an R data set. The R harvesting script from section 2.1 was rebooted to collect historical air temperature data at the time of ECOSTRESS flyover. A .csv file with metadata about the weather station and flyby, as well as data pertaining to land cover type, hillshade, land surface temperature, and surface air temperature, was exported.

2.3 Data Validation in R

After section 2.2 was complete, all .csv files were aggregated into one "master" .csv file, within which the differences between ECOSTRESS land surface temperature and Weather Underground surface air temperature (henceforth called "temperature penalties") were calculated. The final predictor variable to calculate was sun altitude, which was selected over "hour of day" because time ignores seasonal climatic differences due to Earth's tilt and orbit. The *suncalc* library in R was employed to approximate the angle of elevation of the sun at each weather observation by taking latitude, longitude, and time as arguments. After obtaining sun altitude, all predictor variables were accounted for: season (summer, autumn, winter, spring); land cover type (fifteen across Washington, excluding "Snow/Ice"); shadow (yes or no); and sun altitude (grouped every 15° of elevation before and after solar noon), resulting in 1,218 permutations. In R, the average penalty for each permutation was calculated, giving a baseline to start determining spatial-temporal trends in temperature skew.

Two final data validations steps in R helped to strengthen the accuracy of the temperature penalties: outlier removal and bagging (bootstrap aggregating). To remove outliers non-arbitrarily, the penalties data were transformed via a Box-Cox power transformation to the nearest normal-like distribution. Box-Cox transformations are done to non-normally distributed data so that the data more closely meet statistical assumptions of normality (Osborne, 2010) Logarithmic and square-root transformations are simple cases of Box-Cox when its parameter λ equals 0 and 0.5, respectively. The penalties data best represented a normal distribution where $\lambda = 0.693$, which is equivalent to a Gamma ~ (5.85, 0.35). The

Gamma distribution converges to a normal distribution when its two parameters (α, β) approach infinity.

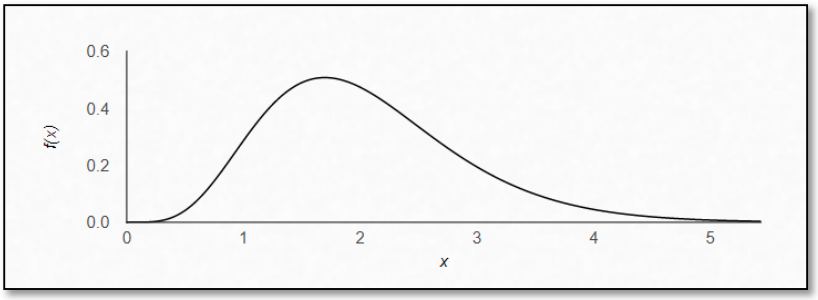

Figure 1. The Gamma ~ (5.85, 0.35) probability density function

With the penalties data now fitting near-normal distribution, it is more appropriate to find outliers by calculating each observation's Cook's Distance (an observation's measure of influence on the shape of the distribution). Those that exceeded the traditional $4/(n\text{-}k\text{-}1)$ criterion (where n is the number of weather observations: 179,623, and k is the number of predictor variables: 4) were removed, leaving 171,697 remaining (Fox 1991).

The second data validation step was bagging (bootstrap aggregating), a supervised learning technique that, among other things, reduces variance of a model. This is not to be confused with improving the model's performance, but rather ensuring the results reflect what should happen if implemented in reality. In a nutshell, bagging replicates the results of a model d times by resampling with replacement a portion of the data ("bootstrapping") and testing it on the remaining samples to produce new penalties. Each dth set of penalties is averaged to produce a bootstrapped mean of penalties, which takes the place of the original penalties. For this project, this process was executed a total of d = 1,000 times. A copy of these penalties is online at https://github.com/ermian98-uw/GIS/blob/main/Capstone/ALL_PENALTIES.csv.

2.4 Data Visualization for Climate Discussion

The final component of this analysis was data visualization via maps. The rasters stored in the file geodatabase in section 2.2 were programmatically merged via Python by variable and mapped to the land cover types of Washington (giving each temperature map a name of "Season_SunAltitude_Shadow"). The bootstrapped penalties from section 2.3 were joined to these rasters according to the variable combination. From these penalties, the ArcGIS Raster Calculator was used to convert the 70x70-meter land surface temperature grids to "air temperature" grids. By completing this step, this project reached its first goal of obtaining and illustrating air temperature within any pixel, regardless if a weather station existing there or not (e.g., within all CLEARCUT pixels, where sun altitude is BETWEEN 30°-45°, in SHADOW, during SUMMER). This was a prerequisite to locating the "hot" and "cold" spots between topographies in Washington state.

To aid the eye in delineating such "hot" and "cold" spots, one last Python script was written to perform nearest-neighbor spatial autocorrelation (SA) on the rasters (to do this, the rasters were first converted to point features). Specifically, the Getis-Ord Gi* Hot Spot Analysis was run, which assigns z-scores to features based on the feature's proximity to clusters of high or low values. Z-scores in the 1st and 99th percentiles were classified as cold and hot spots, respectively. In the interest of time and redundancy, these analyses were limited to the broadest

predictor categories (each season day + night, equalling 8 analyses). The benefit of the Getis-Ord Gi* method is that the z-scores can be intersected with land cover type to produce tables showing the location and magnitude of air temperature skew by predictor variable. Maps and tables such as these are key to fostering broader climate and public health discussions, and key to promoting the research of urban heat islands (UHI) and policymaking surrounding land use land cover (LULC) classification, both of which are discussed below.

3. Literature Review

This project expands upon two well-documented remote sensing subjects: the urban heat island (UHI) effect, and land use land cover (LULC) classification. Despite being used often in micro-scale studies (e.g., studying a single city), the marriage of the two with this project contribute greatly to climate change discussions at large.

3.1 The Urban Heat Island Effect

An urban heat island is a high concentration of thermal radiation in cities and industrial regions compared to outlying cooler rural regions. A critical component of climate change analysis, the UHI effect is by far the most obvious example of localized temperature variation independent of meteorological patterns. Highly urbanized lands contain dark, artificial, carbon-based materials (such as asphalt and other metals) that absorb an astonishing amount of solar radiation, rather than reflecting it back towards the sky as terrestrial radiation (Elmes *et al.* 2020). Thus, these surfaces become energized and ultimately emit the absorbed solar radiation back into the air as heat, raising air temperature. This consequence is augmented further by urban air pollution from machine energy consumption, creating a greenhouse effect that traps the already warm air.

Most research about the urban heat island effect is currently aimed at minimizing city absorption of solar radiation by identifying surfaces with low albedo, or low ratio of reflected solar radiation to incoming solar radiation (Aleksandrowicz *et al.* 2017). Albedo is measured on a scale from zero to one: asphalts and dirt are nearly zero, while forest canopies and snow are near one. Replacing low albedo surfaces with high albedo surfaces is considered a crucial public health measure. Novel solutions are implemented every year, such as: planting gardens of vegetation atop city roofs; planting bushy deciduous trees in dry residential (especially low-income) areas; painting black surfaces white after construction is finished; and strategically unsealing surfaces that generate excess stormwater runoff (Johnson *et al.* 2020). Other researchers focus on improving air quality by designing “zero-heat” or “microclimate neutral” buildings that cut back electricity use and excessive indoor heat emission (He 2019).

Conceptually, this project does not seek to differentiate urban heat islands from rural temperature variation; however, the skewed distribution of terrestrial weather stations favors highly populated areas. Therefore, urban regions will have more data samples to draw from and will yield more statistically robust tests, such as spatial autocorrelation of temperature penalties (surface temperature minus air temperature) for pinpointing homogeneous low albedo (hot) surfaces. Ideally, rural heat variation will still be dramatic enough to warrant discussion about warm overlooked surfaces – natural or synthetic. Regardless, the use of temperature (not albedo) data in this project to describe terrestrial environmental conditions is meant to produce

more visceral results for the average person, who is more familiar with associating heat with degrees Fahrenheit or Celsius.

3.2 Land Use Land Cover Classification

Second, this project incorporates literature about land use and land cover (LULC) classification, particularly rural ecological land. LULC classification is the assignment of pixels in an image file that exhibit similar spectral characteristics to spectral classes via a supervised or unsupervised clustering algorithm. These pixel classes represent various visible features on the Earth's surface (e.g., water, snow, croplands), which, when cross-referenced with how those features are modified by humans, reveal subtle phenomena such as localized temperature variation. For example, land cover and ground moisture are highly correlated in rural areas due to agriculture (this is especially true in Washington), suggesting that minimum and maximum air temperatures per season fluctuate more in rural areas (Lawston *et al.* 2020).

LULC depends significantly on ground-truthing, or the collection of observations about the size, type, condition, and any other important physical or chemical properties concerning the materials on the Earth's surface (Hoffer 1972). Quite often, whether a result of mechanical error or radiometric interference, remotely sensed pixels are misclassified; ignoring this may lead to disastrously incorrect conclusions. A common misclassification (one addressed in the land cover data obtained for this project) is the assignment of water pixels as tree-cast shadows, or vice versa. Verifying a sample of ground features within various pixels of a study area can reveal misclassification patterns across the entire study area and beyond. It also reduces the chance of a classification algorithm assigning improper classes to regions undergoing unprecedented, rapid ecological change (Nagai *et al*. 2020). The validity of classification algorithms is measured by both producer's accuracy (percentage of an LULC type on the ground correctly classified from the map) and user's accuracy (percentage of a class on the map that matches the corresponding class on the ground) (Tran *et al.* 2017). Urban and environmental policymaking rely substantially on this. By judging historical aerial imagery against modern imagery, policymakers can predict what the future environment footprint may look like and apply models such as the one this project seeks to create to estimate climate impact.

3.3 Relevance Towards Climate Change Research

The marriage between the urban heat island effect and LULC classification is inexorable. For example, the normalized difference vegetation index (NDVI), which uses spectral band math to delineate probable areas of vegetation, measures the growing amount of green space in urban areas – this has a negative correlation with surface temperature (Bokaie *et al.* 2016). Appropriately sized, dense, amorphous, and cohesive green patches distributed in clusters around a city (meant to imitate undisturbed nature) most radically disperses urban heat (Kowe *et al.* 2021). Similar normalized indices for other land cover types, combined with cloud cover raster data, has yielded sophisticated statistical techniques that estimate seasonal variability of urban land surface temperature, with greater success across homogenous land cover types (Guha, Govil, & Diwan 2019).

New technologies like the ECOSTRESS experiment, docked with the International Space Station (ISS), make projects studying this crossover increasingly more powerful than previous research. The ECOSTRESS experiment was selected because of its sensor's desirable temporal resolution (90% of CONUS every 4 days), radiometric resolution (8 - 12.5 µm), and excellent spatial resolution (~70-meter) (Cawse-Nicholson & Anderson 2018). Launched into space in

June 2018, the experiment seeks to learn more about how plants use water to regulate temperature, which impacts regional evapotranspiration and indicates whether or not a region may be entering a period of drought (Hulley *et al.* 2015). Despite its emphasis on vegetation, its land surface temperature and emissivity product (ECO2LSTE) is sufficient for measuring temperature across any surface type.

This project acknowledges the depth to which the UHI and LULC crossover has been examined, and incorporates the scientific findings of this crossover. Since 62% of the Weather Underground stations exist on well-developed land, this project supplements existing efforts to mitigate UHI and establish ecologically friendly land cover types. However, it differentiates itself by hypothesizing that pockets of air temperature variation exist everywhere, even if few and far between (rural and urban). This is a less common research angle, as urban areas experience anywhere from 1.4 to 15 times more heat stress than rural areas, justifying the vast body of UHI research (Wouters *et al.* 2017). Yet, as Wouters *et al.* (2017) point out, rural heat stress varies by topography, implying that the UHI effect is not solely responsible for localized air temperature variation. Though minor, non-UHI phenomena may also influence climate patterns; this project strives to pinpoint and quantify the nature of these phenomena in Washington state.

4. Description of Application/Intervention

Three interventions were created as a result of this project: a repository of R and Python code[1], a collection of GIF timelapses[2], and an ArcGIS Web Application[3]. Above all else, these applications are meant to be tools for the user to apply to their own applications of temperature pattern research. The computer code is made available for users who wish to replicate similar results using similar coding strategies, while expounding upon the methods of this project and providing transparency into the methods and results of this project. The GIF timelapses (produced with R) are compact ways to present some of the numerous raster layers spliced together in section 2.4. These are downloadable from the author's portfolio page and presented with a pixel resolution nearly equivalent to the 70x70 meter grid across Washington. Finally, the ArcGIS Web App functions as a sandbox with samples of land surface temperature to surface air temperature variation and hot/cold spots during summer 2020 and winter 2021. It allows a user to confine their study area to any portion of Washington and take note of the skewed (if any) temperatures within that region. This app additionally contains metadata about each of the 171,697 weather observations retained in section 2.3 in order to underscore the varied distribution of stations across the state of Washington and to contextualize how the temperature penalties were derived. To help draw climate impact conclusions, the latter two interventions are structured to illustrate temperature fluctuation between different tested variables (namely, season and sun altitude across land), and are symbolized by familiar temperature color palettes that weather maps frequently employ. See the beginning of the References section for hyperlinks to each intervention.

5. Discussion of Results

Three of the four predictor variables demonstrated substantial uniqueness in temperature penalty distribution, implying they were essential to final model accuracy. The fourth, shadow, did not: results across shadowed and shadowless surfaces were not significantly different by two-sample *t*-test (Table 1). Likely, this is due to poor data quality, as the hillshades generated by the Python script applied solar zenith and azimuth values at the centroid of the ECOSTRESS flyby. At times, these hillshades covered tens of thousands of square miles of Washington state,

whose opposite sides may have been wildly different; for instance, featuring a low-altitude sun versus a setting sun. Additionally, these hillshade models did not account for building shadow, an issue considering that most weather observations were in metropolitan areas.

Table 1. Two-sample comparison test of shadowed and shadowless penalties across all land cover, sun altitude, and season permutations. The high p-value (0.81) suggests that shadowed and shadowless penalties are not significantly different at α = 0.05.

	Shadowed	Shadowless
Mean (μ)	7.235	7.167
Variance (σ^2)	11.20	10.79
n	406	406
t-statistic	0.240	
p-value	**0.810**	

After merging shadowed and shadowless penalties and affixing them to land surface temperatures (LST) to estimate a surface air temperature (SAT) grid, the absolute difference between LST and SAT shrunk by 35.7%, with 69.8% of observations reporting a more accurate SAT than before correction. This is a promising improvement, particularly the latter statistic, which would be 50% if subjected to random chance under an ROC curve (Mas *et al.* 2013). Table 2 breaks down how well the observations were corrected after LST penalty adjustment.

Table 2. Outcomes after adjusting each observation's LST to estimated SAT with its corresponding penalty.

Outcome	Count	Percent
Better, Not Enough	76,476	44.5%
Better, Too Far	43,721	25.2%
Perfect	170	0.1%
Overshot	28,861	16.8%
Wrong Direction	22,919	13.4%
Total	**171,697**	**100.0%**

The absolute difference was measured by each combination of predictor variables, too. Tables 3-5 highlight the best and worst performing variables, single-crossed, double-crossed, and triple-crossed. 100% in the second column denotes a perfect correction; percentages below 50% in the third column imply that random chance would estimate SAT better than the penalty.

Table 3. Improvement towards SAT after affixing penalties to LST, by best/worst-performing single variables. M = morning; A = afternoon.

Variable	% Improvement towards SAT	% Observations Improved
Cultivated Crops	52.2%	77.9%
Winter	47.5%	75.9%
0° - 15° (A)	47.0%	76.8%
Autumn	31.8%	68.9%
Open Water	16.0%	60.7%
15° - 30° (A)	4.4%	53.7%
Total	**35.7%**	**69.8%**

Table 4. Improvement towards SAT after affixing penalties to LST, by best/worst-performing double variables. M = morning; A = afternoon.

Variables	% Improvement towards SAT	% Pixels Improved
Winter, Woody Wetlands	66.7%	87.7%
0° - 15° (A), Cultivated Crops	65.2%	87.7%
45°+ (M), Developed High Intensity	64.2%	86.1%
15° - 30° (A), Herbaceous	0.9%	50.3%
15° - 30° (A), Developed Low Intensity	0.3%	50.2%
30° - 45° (A), Open Water	-6.9%	45.4%
Total	**35.7%**	**69.8%**

Table 5. Improvement towards SAT after affixing penalties to LST, by best/worst-performing triple variables. M = morning; A = afternoon.

Variables	% Improvement towards SAT	% Pixels Improved
Summer, 45°+ (M), Developed Medium Intensity	67.6%	90.4%
Summer, 45°+ (M), Cultivated Crops	66.8%	88.3%
Autumn, 0° - 15° (A), Cultivated Crops	64.6%	88.7%
Summer, 15° - 30° (A), Herbaceous	-1.5%	47.8%
Spring, 15° - 30° (M), Developed Low Intensity	-1.8%	45.9%
Spring, 15° - 30° (M), Developed Medium Intensity	-2.0%	46.0%
Total	**35.7%**	**69.8%**

Beyond the top three, observations with season equal to summer, sun altitude greater than 45°, and developed land cover, were best corrected by the penalties. This further exposes the extent to which urban heat islands skew temperature. Beyond the worst three, observations with season equal to spring, sun altitude equal to 15° - 30°, and the lightly forested or floral land cover, were the least corrected (and occasionally worsened) by the penalties. Overall, the better-performing variable combinations were more numerous in this study because cloud cover was less prevalent (Table 6). For instance, observations after solar noon outnumbered those before solar noon 62,004 to 38,250. This is one potential source of bias, as these combinations are geographically uncommon in Washington state, which sees sun altitude greater than 45° during a short time of the year and is composed of less than 10% urban-developed land (derived from Wickham *et al.* 2021). The opposite was true for the worse-performing variables.

Table 6. Number of Weather Observations by Season and Sun Altitude. M = morning; A = afternoon.

Season / Sun Altitude	Count	Percent
Autumn	41,851	24.4%
Spring	45,592	26.6%
Summer	66,476	38.6%
Winter	17,778	10.4%
Sun Beneath Horizon	71,443	41.6%

0° - 15° (M)	8,421	4.9%
15° - 30° (M)	8,558	5.0%
30° - 45° (M)	7,864	4.6%
45° or higher (M)	13,407	7.8%
45° or higher (A)	17,459	10.1%
30° - 45° (A)	12,024	7.0%
15° - 30° (A)	15,405	9.0%
0° - 15° (A)	17,116	10.0%
Total	**171,697**	**100.0%**

Although the hot spot analysis was done primarily for visualization purposes, it is worth noting the correlations between various land cover types and hot/cold spots (Table 7). In the table below, the land cover types are sorted by greatest SAT difference between day and night. By doing this, the reader will notice which land cover types overwhelmingly contain hot spots during the daytime versus during the nighttime. For example, Woody Wetlands and Hay/Pasture were relatively hot land cover types during the day, but relatively cold during the night. The opposite was true for Barren Land, Cultivated Crops, and Open Water, which were hotter relative to their surroundings at night. All developed/urban land types were equally hot during the day and night relative to their surroundings, with 84% of its area deemed a hot spot during the day, and 81% at night.

Table 7. Tendency towards a pixel assignment of SAT "hot spot", Washington State. Scores of 1.0 indicate overwhelmingly hot during the day; -1.0 during the night.

Land Cover Type	Summer	Autumn	Winter	Spring	Annual Average
Woody Wetlands	0.63	0.52	0.50	0.17	**0.45**
Hay/Pasture	0.78	0.42	0.31	0.26	**0.44**
Emergent Herbaceous Wetlands	0.60	-0.20	0.26	0.14	**0.24**
Evergreen Forest	0.45	0.20	0.00	0.20	**0.21**
Herbaceous	0.24	-0.10	0.21	0.30	**0.16**
Developed, Open Space	0.24	0.06	0.10	0.12	**0.11**
Mixed Forest	0.24	0.22	-0.39	0.16	**0.06**
Shrub/Scrub	0.17	-0.07	-0.06	0.08	**0.03**
Developed, Low Intensity	-0.07	0.11	0.05	0.02	**0.03**
Developed, Medium Intensity	0.03	-0.04	-0.04	0.02	**-0.01**
Developed, High Intensity	0.00	-0.01	-0.04	-0.01	**-0.00**
Deciduous Forest	0.07	0.15	-0.33	-0.03	**-0.04**
Barren Land	0.07	-0.23	0.00	-0.04	**-0.05**
Cultivated Crops	-0.29	-0.60	-0.48	-0.22	**-0.40**
Open Water	-0.91	-0.72	-0.23	-0.91	**-0.69**

The outcomes of this outlier detection of SAT hot/cold spots could be improved by calculating outliers within smaller zones. In this analysis, the Getis-Ord Gi* Hot Spot Analysis was done within county boundaries, meaning each counties' hot/cold spots were considered the state's hot/cold spots. This is preferable over zoneless analysis, which would simply output the hottest/coldest part of the state. However, counties are political boundaries that do not always follow topography. Thus, applying the Getis-Ord Gi* Hot Spot Analysis to smaller,

squarer, and perhaps more randomized zones, would allow convergence towards the truest hot/cold spots.

One fascinating instance of many, implied by Table 7, is illustrated in Figures 2 and 3 below. The maps depict average SAT (as estimated by this project's penalties) during summer daytime and summer nighttime for rural eastern Washington, near the towns of Ritzville and Odessa. These regions are rich with farmland, some of which is frequently irrigated and cultivated, and some of which is left dry, grassy, and uncultivated. The ECOSTRESS sensor picked up on this difference, recording vastly different LSTs during the day. Thus, even after temperature penalty correction to SAT, the hot spot analysis picked out the moist lands as possessing cold SAT relative to their surroundings. The story was reversed at night, though, with moist lands (in this case, Sylvan Lake and other low-lying, creek-riddled areas) possessing hot SAT relative to their surroundings. This is a fascinating example of pinpointing of LST and SAT variability across topographies in a subsection of Washington during day and night.

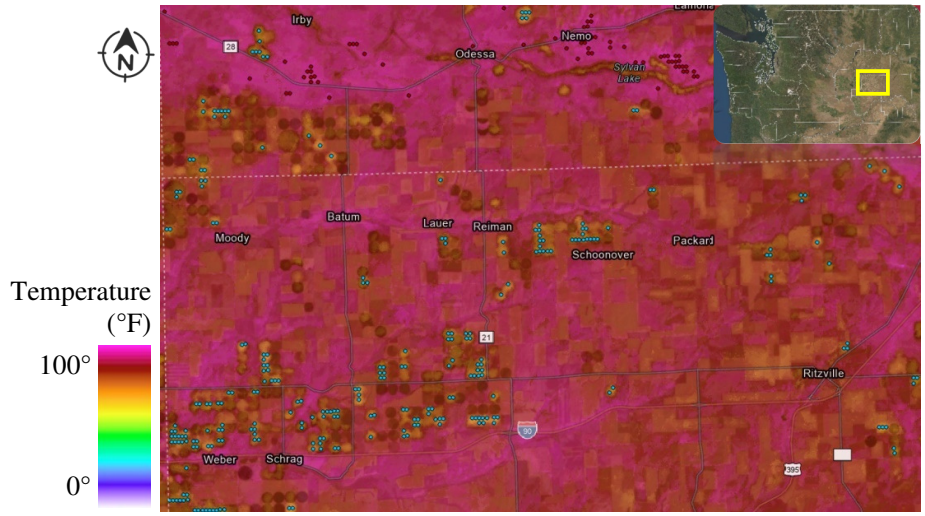

Figure 2. Region of eastern WA with daytime summer SAT and hot/cold spots. Red dots are hot spots (99th %ile regional SAT); blue dots are cold spots (1st %ile regional SAT).

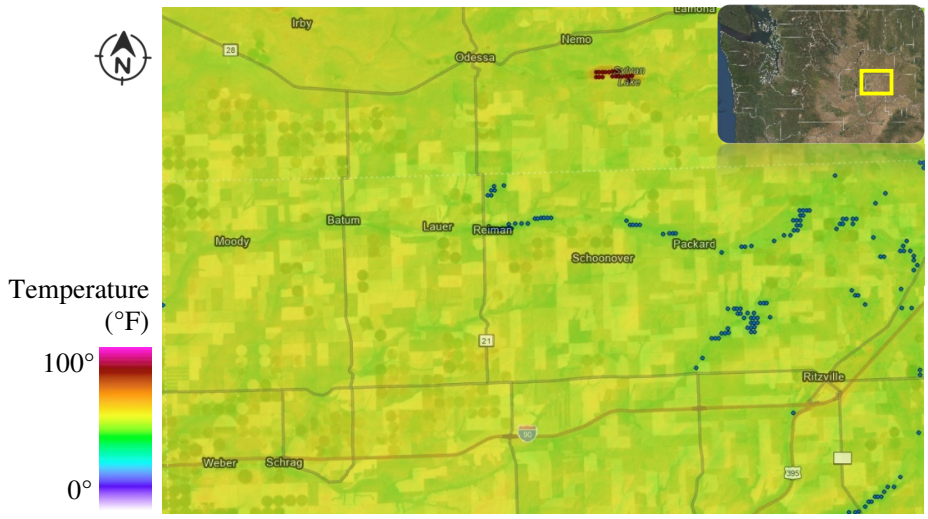

Figure 3. Region of eastern WA with night summer SAT and hot/cold spots. Red dots are hot spots (99th %ile regional SAT); blue dots are cold spots (1st %ile regional SAT).

As mentioned before, the enormity of the urban heat island (UHI) effect was echoed by the results of this project. Perhaps necessarily, this project specifies that the UHI effect is prominent during day hours, not night hours (though it still exists at night). This is portrayed in Figures 4 and 5, which show average SAT (as estimated by this project's penalties) during spring daytime and spring nighttime. The subject is the modest town of Sequim, WA (on the Olympic Peninsula of western Washington). Sequim was chosen given its relative remoteness to other developed cities, and its nearness to both large mountains and bodies of water. From Figures 4 and 5, it is evident that daytime SAT suddenly shifts warm in even the smallest urban settings, as opposed to nighttime SAT, which is more homogenous across urban settings and warmer in enclosed deciduous forest land. The configuration of hot spots in Figures 4 and 5 were consistent with many suburban regions across the state of Washington.

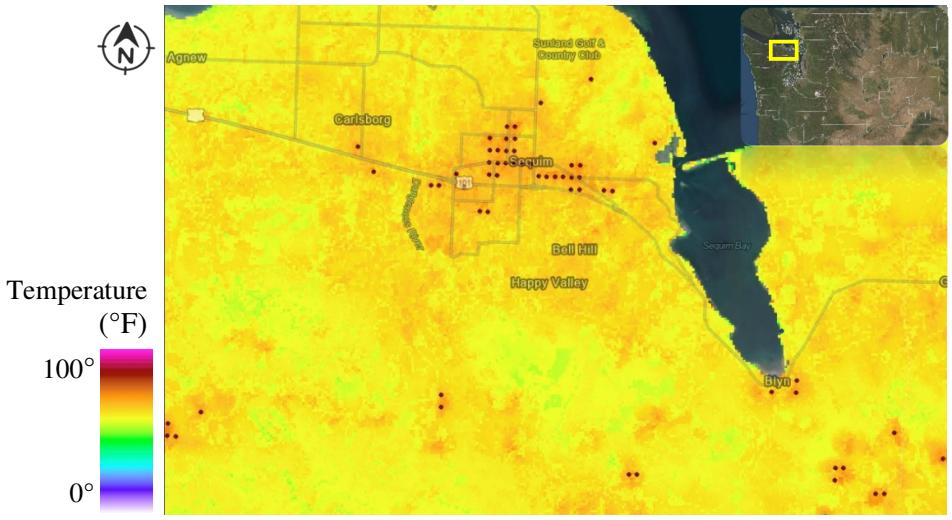

Figure 4. Vicinity of Sequim, WA with daytime spring SAT and hot/cold spots. Red dots are hot spots (99th %ile regional SAT); blue dots are cold spots (1st %ile regional SAT).

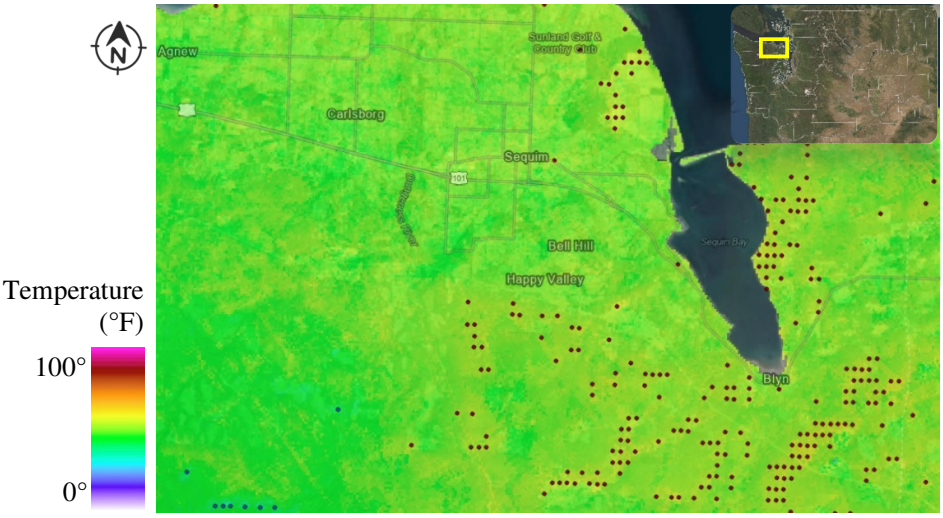

Figure 5. Vicinity of Sequim, WA with night spring SAT and hot/cold spots. Red dots are hot spots (99th %ile regional SAT); blue dots are cold spots (1st %ile regional SAT).

Remember that the figures depict SAT after penalties were applied to LST, not LST itself.

6. Conclusion

By blending the advantages of spaceborne and terrestrial temperature data, this project created a semi-robust model of "temperature penalties" that estimated surface air temperature (SAT) variation across the topographically diverse state of Washington. Such an algorithm could be coded into digital weather apps for public use, and also coded into rigorous climate analyses that aim to pinpoint phenomena that contribute to global warming. Exploiting the knowledge of these corrections may enable future researchers to model temperature when localized data is unavailable.

Upon viewing the maps in this paper and in the interventions, one will see that SAT patterns still mimic LST patterns; in other words, there is no appreciable visual difference. Because the absolute difference was improved by merely 35.7%, this could be explained several ways but remains inconclusive. First, perhaps SAT *does* mimic LST, in the sense that a person touching, for example, a hot urban surface versus a cold irrigated pasture will be simultaneously breathing hotter air two meters above the ground at that urban surface. Or perhaps SAT *does not* mimic LST, contrary to these findings, and the 35.7% correction is simply inaccurate or insufficient to reveal the true SAT pattern. Again, it is worth reiterating that rural area penalties performed worse than urban area penalties, so the 35.7% statistic overestimates rural improvements and therefore overestimates what a map shows (since rural lands comprise 90%+ of Washington). This warrants a plea to install or manage more rural weather stations, or procure more ground-truth data by physically verifying the SAT *and* LST of a particular set of sites.

Furthermore, more accurate results may materialize by accounting for other atmospheric effects, such as humidity and wind, which are two contributors to climate change that would more strictly differentiate urban from rural. This would also help address a more interpersonal aspect of temperature. Humans react to temperature differently than a thermometer does, which becomes obvious when we think about the "feels like" temperature versus raw outdoor temperature. These alternative indices, themselves a correction analogous to this project's temperature penalties, combine temperature with ambient atmospheric effects like humidity and wind to better inform citizens of local weather. This is important to consider if applying penalties is meant to inform citizens, too, because LST does not have the same "feels like" component as SAT does.

Additionally, it is important to reiterate that the results of this project apply only to cloudless skies. Atmospheric disruptions, such as cloud cover, are a grave handicap of remote sensing research in general. However, in recent years, researchers have proposed workarounds to reasonably estimate LST during cloudy conditions, including: accounting for the solar-cloud-satellite geometry effect, through which clouded LSTs of shadowed and illuminated pixels are estimated (Wang *et al.* 2019); and, measuring the diurnal evolution of temperature and net shortwave solar radiation (NSSR) against surface temperatures (Zhang, Pang, & Li 2015). These various bodies of research point towards evidence that the disparity between LST and SAT is much smaller under cloudy or overcast conditions, since the industrial and atmospheric greenhouse effect is weaker without direct sunlight. Under cloudless skies, SAT (especially in heavily developed flat land) swings from hot to cold over the course of one day more prominently than under cloudy skies, due to a diminished greenhouse effect.

Other types of future research could expand upon this project in multiple ways. First, remedies exist to offset the fact that the ECOSTRESS experiment requires nearly 100 hours to probe the contiguous United States, while terrestrial weather stations provide 5-minute updates.

It might be valuable to mirror this project's procedure using data from a higher temporal, lower spatial resolution satellite like MODIS, and extract temperature penalties from a much wider region of space. Even though MODIS obtains data on a 250x250-meter grid, one could resample to match the 70-meter ECOSTRESS grid, since land cover, etc. is obtainable at such a resolution. In this scenario, land surface temperature would be coarser with most of the 70x70-meter cells matching one another, but the penalties would still be applied at their proper coordinates and offer unique temperature values. Using one or multiple different satellites would help overcome the issue of intermittent coverage/flybys. Second, historical LULC data sets could be juxtaposed with the 2016 data set used in this project to ascertain how disparate surface air temperature may have been if land were being used differently today. For instance, research documents the ways that deforested clearcut areas exacerbate soil runoff and species habitation over time (Dymov, 2017). The same may be true for surface air temperature.

References

1 https://github.com/ermian98-uw/GIS/tree/main/Capstone
2 https://ermian98-uw.github.io/GIS/Anderson_Lab5/capstone.html
3 https://uwt-gis-geo-hub.maps.arcgis.com/apps/webappviewer/index.html?id=f6c2b70cd8604a73a1c0a81b9b50a2da

4 https://git.earthdata.nasa.gov/projects/LPDUR/repos/ecostress_swath2grid/browse
5 https://www.wunderground.com/pws/overview

Aleksandrowicz, Or, Milena Vuckovic, Kristina Kiesel, and Ardeshir Mahdavi. "Current trends in urban heat island mitigation research: Observations based on a comprehensive research repository." *Urban Climate* 21 (2017): 1-26.

Blachowski, Jan. "Introduction to GIS spatial analysis." Lecture, Wrocław University of Science and Technology, Department of Mining and Geodesy, Wrocław, Poland, October 28, 2019.

Bokaie, Mehdi, Mirmasoud Kheirkhah Zarkesh, Peyman Daneshkar Arasteh, and Ali Hosseini. "Assessment of urban heat island based on the relationship between land surface temperature and land use/land cover in Tehran." *Sustainable Cities and Society* 23 (2016): 94-104.

Cawse-Nicholson, Kerry, and Martha C. Anderson. "ECOsystem Spaceborne Thermal Radiometer Experiment on Space Station (ECOSTRESS) Mission." (2018).

Cristóbal, Jordi, M. Ninyerola, and Xavier Pons. "Modeling air temperature through a combination of remote sensing and GIS data." *Journal of Geophysical Research: Atmospheres* 113, no. D13 (2008).

Dymov, A. A. "The impact of clearcutting in boreal forests of Russia on soils: a review." *Eurasian Soil Science* 50, no. 7 (2017): 780-790.

Eliezer, Heather, Sarah Johnson, William L. Crosson, Mohammad Z. Al-Hamdan, and Tabassum Z. Insaf. "Ground-truth of a 1-km downscaled NLDAS air temperature product using the New York City Community Air Survey." *Journal of Applied Remote Sensing* 13, no. 2 (2019): 024516.

Elmes, A., M. Healy, N. Geron, M. M. Andrews, J. Rogan, D. G. Martin, F. Sangermano, C. A. Williams, and B. Weil. "Mapping spatiotemporal variability of the urban heat island across an urban gradient in Worcester, Massachusetts using in-situ Thermochrons and Landsat-8 Thermal Infrared Sensor (TIRS) data." *GIScience & Remote Sensing* 57, no. 7 (2020): 845-864.

Fox, John. (1991). *Regression Diagnostics: An Introduction*. Sage Publications.

Guha, Subhanil, Himanshu Govil, and Prabhat Diwan. "Analytical study of seasonal variability in land surface temperature with normalized difference vegetation index, normalized difference water index, normalized difference built-up index, and normalized multiband drought index." *Journal of Applied Remote Sensing* 13, no. 2 (2019): 024518.

He, Bao-Jie. "Towards the next generation of green building for urban heat island mitigation: Zero UHI impact building." *Sustainable Cities and Society* 50 (2019): 101647.

Hoffer, Roger M. "The importance of ground truth data in remote sensing." The Laboratory for Applications of Remote Sensing, Purdue University (1972).

Hulley, Glynn, Sarah Shivers, Erin Wetherley, and Robert Cudd. "New ECOSTRESS and MODIS land surface temperature data reveal fine-scale heat vulnerability in cities: A case study for Los Angeles County, California." *Remote Sensing* 11, no. 18 (2019): 2136.

Johnson, Daniel, Linda See, Sandro M. Oswald, Gundula Prokop, and Tamás Krisztin. "A cost–benefit analysis of implementing urban heat island adaptation measures in small-and medium-sized cities in Austria." *Environment and Planning B: Urban Analytics and City Science* (2020): 2399808320974689.

Kowe, Pedzisai, Onisimo Mutanga, John Odindi, and Timothy Dube. "Effect of landscape pattern and spatial configuration of vegetation patches on urban warming and cooling in Harare metropolitan city, Zimbabwe." *GIScience & Remote Sensing* (2021): 1-20.

Lawston, Patricia M., Joseph A. Santanello Jr, Brian Hanson, and Kristi Arsensault. "Impacts of Irrigation on Summertime Temperatures in the Pacific Northwest." *Earth Interactions* 24, no. 1 (2020): 1-26.

Mas, Jean-François, Britaldo Soares Filho, Robert Gilmore Pontius, Michelle Farfán Gutiérrez, and Hermann Rodrigues. "A suite of tools for ROC analysis of spatial models." *ISPRS International Journal of Geo-Information* 2, no. 3 (2013): 869-887.

Matthew Quick and Hui Luan. "The spatial structure of socioeconomic disadvantage: a Bayesian multivariate spatial factor analysis." *International Journal of Geographical Information Science* 35, no. 7 (2021): 63-83.

Nagai, Shin, Kenlo Nishida Nasahara, Tomoko Kawaguchi Akitsu, Taku M. Saitoh, and Hiroyuki Muraoka. "Importance of the Collection of Abundant Ground-Truth Data for Accurate Detection of Spatial and

Temporal Variability of Vegetation by Satellite Remote Sensing." *Biogeochemical Cycles: Ecological Drivers and Environmental Impact* (2020): 223-244.

Osborne, Jason. "Improving your data transformations: Applying the Box-Cox transformation." *Practical Assessment, Research, and Evaluation* 15, no. 1 (2010): 12.

Sugita, M., and W. Brutsaert. "Comparison of land surface temperatures derived from satellite observations with ground truth during FIFE." *International Journal of Remote Sensing* 14, no. 9 (1993): 1659-1676.

Tran, Duy X., Filiberto Pla, Pedro Latorre-Carmona, Soe W. Myint, Mario Caetano, and Hoan V. Kieu. "Characterizing the relationship between land use land cover change and land surface temperature." *ISPRS Journal of Photogrammetry and Remote Sensing* 124 (2017): 119-132.

Venter, Zander S., Oscar Brousse, Igor Esau, and Fred Meier. "Hyperlocal mapping of urban air temperature using remote sensing and crowdsourced weather data." *Remote Sensing of Environment* 242 (2020): 111791.

Wang, Tianxing, Jiancheng Shi, Ya Ma, Letu Husi, Edward Comyn-Platt, Dabin Ji, Tianjie Zhao, and Chuan Xiong. "Recovering land surface temperature under cloudy skies considering the solar-cloud-satellite geometry: Application to MODIS and Landsat-8 data." *Journal of Geophysical Research: Atmospheres* 124, no. 6 (2019): 3401-3416.

Wickham, James, Stephen V. Stehman, Daniel G. Sorenson, Leila Gass, and Jon A. Dewitz. "Thematic accuracy assessment of the NLCD 2016 land cover for the conterminous United States." *Remote Sensing of Environment* 257 (2021): 112357.

Wouters, Hendrik, Koen De Ridder, Lien Poelmans, Patrick Willems, Johan Brouwers, Parisa Hosseinzadehtalaei, Hossein Tabari, Sam Vanden Broucke, Nicole PM van Lipzig, and Matthias Demuzere. "Heat stress increase under climate change twice as large in cities as in rural areas: A study for a densely populated midlatitude maritime region." *Geophysical Research Letters* 44, no. 17 (2017): 8997-9007.

Yates, H. W. "A general discussion of remote sensing of the atmosphere." *Applied Optics* 9, no. 9 (1970): 1971-1975.

Zhang, Xiaoyu, Jing Pang, and Lingling Li. "Estimation of land surface temperature under cloudy skies using combined diurnal solar radiation and surface temperature evolution." *Remote Sensing* 7, no. 1 (2015): 905-921.